Title

Large-Scale Testing of the Static One-Dimensional Compression Response of Tire-Derived Aggregate

Authors

Yarahuaman, Axel
McCartney, John S

Publication Date

2023-03-23

DOI

10.1061/9780784484685.060

Large-Scale Testing of the Static One-dimensional Compression Response of Tire-Derived Aggregate

Axel Yarahuaman[1], S.M. ASCE; and John S. McCartney[2], Ph.D., P.E., F. ASCE

[1]Graduate Research Assistant, Department of Structural Engineering, University of California, San Diego, La Jolla, CA 92093-0085; Email: ayarahua@ucsd.edu
[2]Professor and Chair, Department of Structural Engineering, University of California, San Diego, La Jolla, CA 92093-0085; Email: mccartney@ucsd.edu

ABSTRACT

Tire-derived aggregate (TDA) has been adopted in multiple civil engineering applications as a lightweight fill that has the additional benefit of being a recycled material. While the compression response of TDA with small particle sizes has been studied in the literature, there is a lack of data on the response of Type B TDA with larger particles having a maximum dimension of 300 mm. This study focused on assessing the one-dimensional compression response of an 810 mm-thick layer of Type B TDA under quasi-static uniaxial compressive stresses in a large-scale rigid container having a length of 5,029 mm and a width of 2,184 mm. First, this paper presents the results of one-dimensional compression response of Type B TDA under a constant rate of strain test up to a vertical effective stress of 20.4 kPa, which was then maintained for 1 hour to evaluate the creep response. A bi-log-linear compression curve fitted to the nonlinear compression curve for Type B TDA had compression and recompression indices of 0.32 and 0.04, respectively, that are greater than those of most soils. A modified secondary compression index of 0.0029 was observed during creep testing, which is within the range obtained from past TDA studies.

INTRODUCTION

The population growth and transportation system expansion in California and elsewhere in The United States generate an exponential increase in the number of disposed waste tires (CalRecycle 2016a; Edeskar 2004). Research studies have found that waste tires can be recycled and used for civil engineering projects in the shape of tire-derived aggregate (TDA) as embankment material (Meles et al. 2013). Multiple studies have been conducted to assess the feasibility and measure the engineering properties of TDA as a lightweight fill material in embankments or backfill behind retaining walls (Drescher and Newcomb 1994; Hoppe 1994; Tweedie et al. 1998; Humphrey 2008a; Mills and McGinn 2010; Tandon et al. 2007). These studies concluded that TDA has a similar or better performance than conventional fill soils (Humphrey et al. 1992, Bosscher et al. 1993; Hoppe 1998; Dickson et al. 2001), with the additional advantage of its unit weight as low as 5-9 kN/m^3, which is about 33-50% of most granular backfill soils (Ghaaowd et al. 2017).

The two main categories of TDA described by ASTM D6270 and used in practice are Type A TDA, with particle sizes ranging from 75-100 mm, and Type B TDA, with particle sizes ranging from 150-300 mm. The Type B TDA is more cost-effective because it requires less processing than the Type A TDA. Type B TDA layers can also be up to 300 mm-thick while Type A TDA

layers can reach only 100 mm of thickness (ASTM 2012). Although these reasons promote the use of Type B TDA in practice, the uncertainties of the material behavior increase with its larger particles due to the limitations in the size, load, and displacement capability of testing devices.

Only a few studies were conducted to understand the one-dimensional compression behavior of large-sized TDA. Meles et al. (2013) performed compression tests on TDA with sizes of 38 to 150 mm in a large-scale cell with an inside diameter about four times larger than the largest TDA particle. The results indicated a log-linear stress-strain relationship under one-dimensional compression stresses. Ghaaowd et al. (2017) conducted direct shear tests on Type B TDA using a large-scale shearing device designed by Fox et al. (2017), which had a minimum interior dimension of approximately four times larger than the largest TDA particles. The results also suggested a log-linear stress-strain relationship with a compression index C_c of 0.8 for the Type B TDA. However, their compression curve was defined from the initial void ratios from multiple direct shear tests performed under different normal stresses.

The one-dimensional compression tests on Type B TDA presents a challenge to measure as the container size should ideally be ten times or larger than the particle size (ASTM 2011). Meles et al. (2013) and Ghaaowd et al. (2017) used containers with inside dimensions only up to 4 times the larger TDA size. Consequently, this study assesses the one-dimensional compression behavior of Type B TDA in a container with a minimum dimension of 7.3 times the largest Type B TDA particle size. The large-scale testing conditions could improve the understanding of the stress-strain relationship and the particle interlocking behavior for the Type B TDA. The study also attempts to compare a bi-log-linear compression curve and validate its use for TDA with the compression and recompression indices obtained from the experimental data. Another objective of this study is to assess the creep response of the Type B TDA using the large-scale container.

MATERIALS

As previously mentioned, Type B TDA is composed of recycled waste tires shredded to a size ranging from 150 to 300 mm (Ghaaowd et al. 2017). This study considered Type B TDA materials supplied directly by CalRecycle, San Diego. Visual observations of 12 randomly selected TDA particles were carried out to examine the shape, dimensions, and thickness of the material as shown in Figure 1. The particles are flat and irregular with one plan dimension being greater than the other. The particle size information for the Type B TDA evaluated in this study is shown in Table 1. The mean thickness of the particles is 19 mm. Ghaaowd et al. (2017) obtained a specific gravity of 1.15 by weighing a porous plastic bag of Type B TDA in air and submerged in water.

Figure 1. Example of Type B TDA particles.

Table 1. Particle size information for Type B TDA material

Parameter	Longest side	Shortest side
Max. [mm]	241	108
Min. [mm]	44	25
Median [mm]	102	80
Mean [mm]	123	71
Standard deviation [mm]	63	31

EXPERIMENTAL DESIGN

The experimental program was designed to assess the one-dimensional compression behavior of an 810 mm-thick layer of Type B TDA. A compression test was conducted on a large-scale oedometer built at the UCSD Powell Lab using 4 blocks of reinforced concrete walls 254 mm thick as well as one side of the existing strong wall of the lab as shown in Figure 2. Two 5,029 mm long, and 3,048 mm high blocks compose the east and west sides of the container. One 350 mm × 1,575 mm block composes the bottom of the north side of the oedometer. One 6,350 mm × 1,473 mm block composes the top of the north side of the oedometer. The south side of the container consists of portion of the existing strong wall 1000 mm thick from the lab. All reinforced concrete blocks were anchored to the strong floor and wall using high tension bolts and steel chains. The resulting large-scale oedometer has inside dimensions of 5,029 mm × 2,184 mm in plan and a height of 3,048 mm, with adequate capacity to restrain the lateral displacement of the TDA under one-dimensional compression as shown in Figure 2(d).

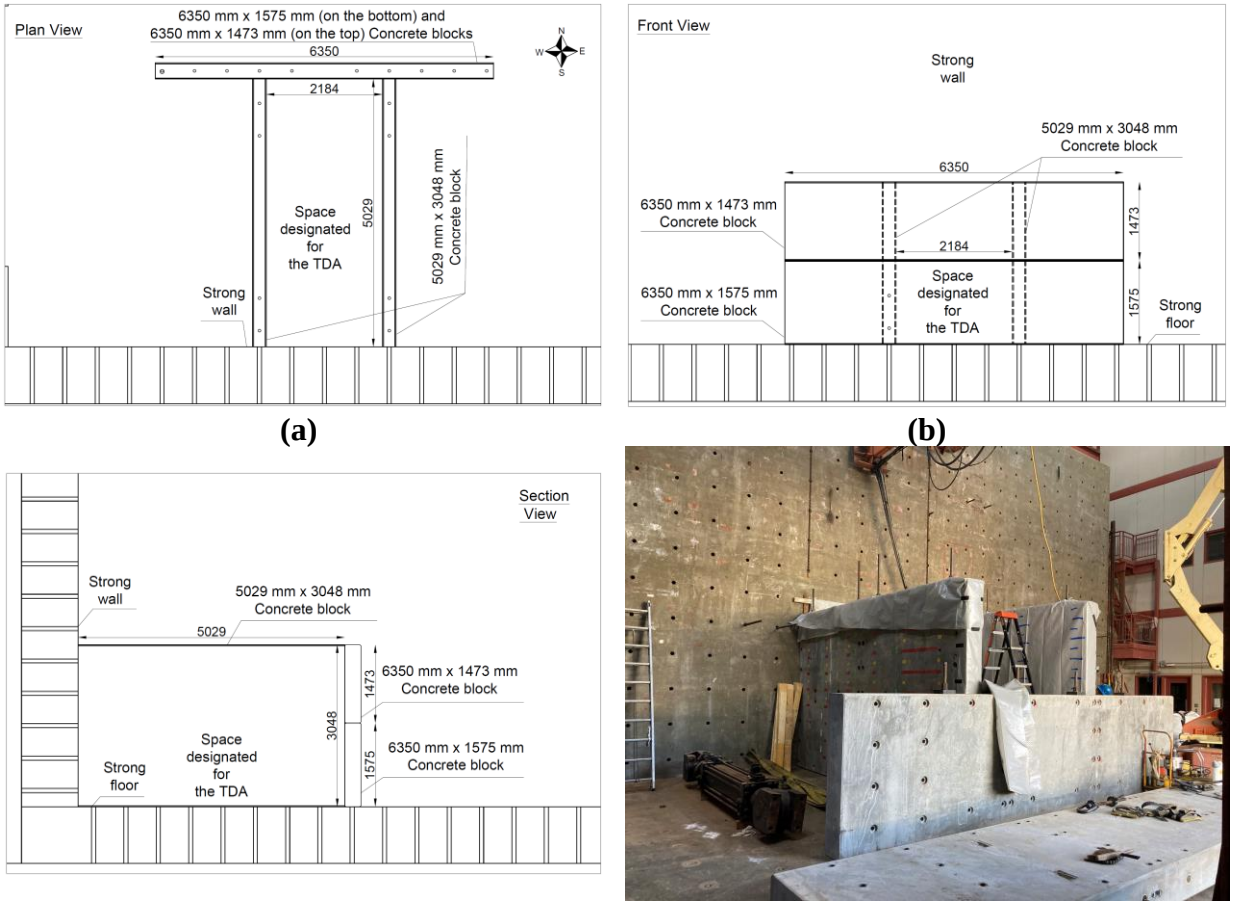

Figure 2. TDA container: (a) Plan view, (b) Front view, (c) Side view, and (f) Picture of oedometer under construction.

One-dimensional compression tests require minimizing the friction between the TDA particles and the inner surface of container so that the externally applied stress is uniform across the depth of the TDA layer. This study followed the approach considered by Yarahuaman and McCartney

(2022) and implemented two layers of thin polyethylene sheet having a thickness of 60 mils (on each side) to cover the inner walls to represent a low-friction interface. The Type B TDA specimen was placed inside the oedometer and compacted uniformly to a dry unit weight of 4.71 kN/m^3. The loading system, which is explained in the following paragraph, was then set on top of the TDA specimen.

The loading system consists of a steel diagonal braced reaction frame, a hydraulic actuator, an actuator mounting plate, and a reinforced concrete platen, as shown in Figure 3. The hydraulic actuator has a static capacity of 222 kN. The platen has dimensions of 5,395 mm × 2,130 mm and a thickness 285 mm. The diagonal braced reaction frame is fixed to the strong wall as a support for the actuator. One end of the actuator is attached to the reaction frame by four bolts. The other end of the actuator is fixed to the actuator mounting plate. The mounting plate allows the connection between the actuator and the platen. The objective of the platen is to distribute the vertical load uniformly on the TDA.

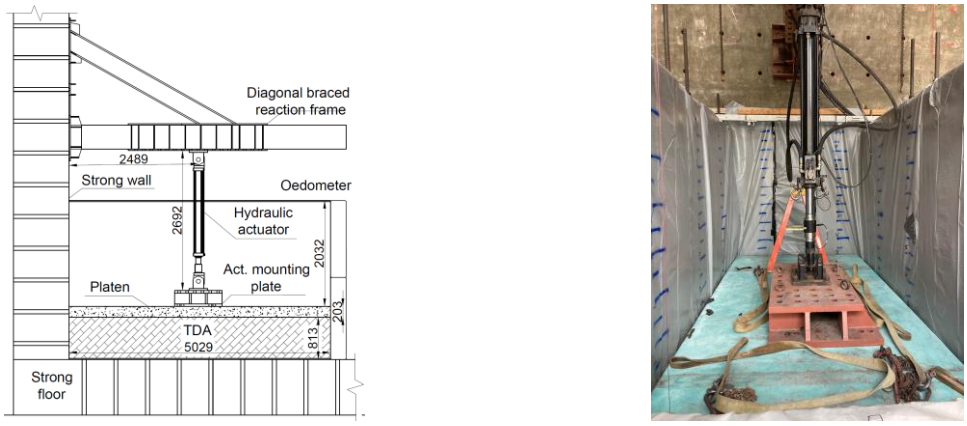

(a) **(b)**

Figure 3. Loading system with units in mm: (a) Elevation section view, and (b) Picture of loading system.

INSTRUMENTATION

A schematic showing instrumentation in the TDA specimen is presented in Figure 4. Spring-loaded linear potentiometers were placed vertically near to the corners of the platen to measure the TDA settlements. Potentiometers P01, P02, P03, P04 (sketched in Figure 4) are used to monitor the north-east, north-west, south-east, and south-west locations, respectively. Aluminum rails were mounted across the top of the oedometer to mount instrumentation.

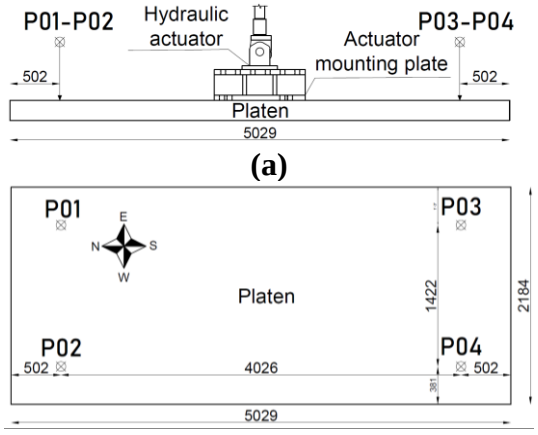

Figure 4. Instrumentation layout with units in mm: (a) Side view, and (b) Plan view

RESULTS

One-Dimensional Compression

Although multiple sets of experiments were conducted on the large-scale oedometer, this paper reports only a single experiment performed to study the compression behavior of the Type B TDA compacted to a dry unit weight of 4.71 kN/m^3. The test protocol consisted of the load-control application of a vertical monotonic load up to 222 kN at a load rate of 222 kN/hr. When the load reached its maximum value, the load was hold constant for 1 hr. After that, the specimen was unloaded following a rate of -222 kN/hr down to 5 kN. The results indicate that the maximum vertical effective stress reached was 20.4 kPa. The potentiometer time-history records indicate that the displacement of the platen is uniform and remains level which indicates that the TDA settled uniformly around the entire plan area of the oedometer. Figure 5 also shows that that creep occurs during the constant load stage. The one-dimensional compression behavior of the TDA is plotted in Figure 5 in terms of stress-strain (natural scale) and stress-void ratio (log-scale) relationships. The stress-void ratio curve shows an example of the Casagrande method to obtain the compression index C_C and recompression index C_r as typically considered for soils.

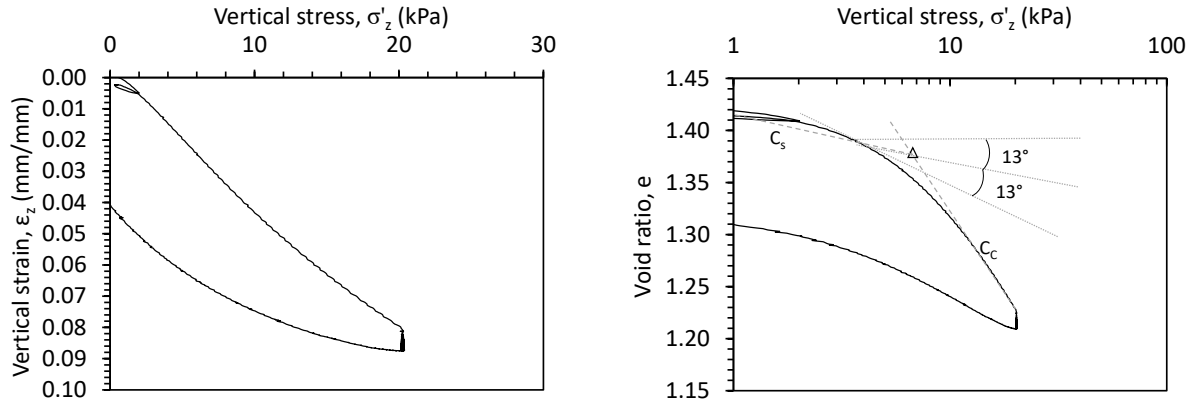

Figure 5. Type B TDA response: (a) Stress-strain curve, and (b) Stress-void ratio curve

The results in Figure 5 reveal a non-linear compression response of the TDA during loading and unloading that is similar in some ways to soils. The compression of the specimen is attributed to the void volume reduction and not to the compressibility of the TDA particles themselves due to relatively low normal stresses and the low volume compressibility of rubber as indicated by a Poisson's ratio of approximately 0.5 (Feng and Sutterer 2000). The stress-void ratio curve illustrates a log-linear behavior with an apparent yield stress that can be found from the maximum curvature when the stress is plotted on a log scale. A slight change in slope is observed for the compression curve is plotted on a natural scale as well. The obtained apparent yield stress σ'_c, compression index C_c, and recompression index C_r obtained from the compression curve in Figure 5(b) were 6.80 kPa, 0.32 and 0.04, respectively. The compression response of the TDA is compared to other similar studies on Type A and Type B TDA as shown in Figure 6.

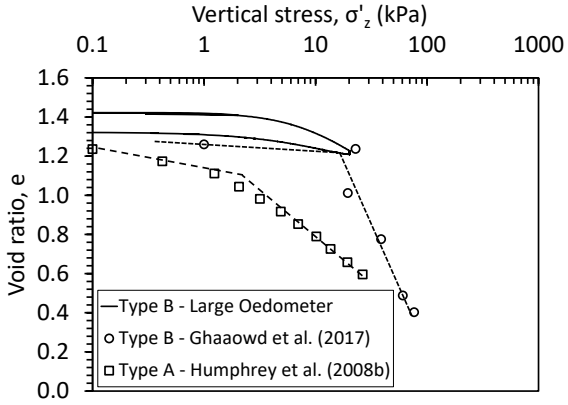

Figure 6. Comparison of stress-strain curves of Type A and Type B TDA

Ghaaowd et al. (2017) found a log-linear Type B TDA compressibility with C_c = 0.80 and C_r = 0.03 at an initial unit weight of 6.00 kN/m^3 under vertical effective stress up to nearly 80 kPa as presented in Figure 6. The comparison confirms the initial compression stage behavior observed in this study because the swell indices are similar. Nonetheless, the C_c computed by Ghaaowd et al. (2017) is 150% larger than the C_c obtained in this study during compression. This difference indicates that the compressibility behavior is highly dependent of the vertical effective stressed induced in the Type B TDA. In other words, Type B TDA under vertical effective stresses larger than 20 kPa can yield to higher compressibility index as shown by Ghaaowd et al. (2017). In addition, Humphrey et al. (2008b) found a log-linear compressibility with C_c = 0.45 and C_r = 0.10 for Type A TDA at an initial unit weight of 5.04 kN/m^3 under vertical effective stress up to nearly 27 kPa, as shown in Figure 6. This comparison indicates that Type B TDA is less compressible during the initial compression stage and more compressible during the initial loading stage than Type A TDA under vertical effective stresses larger than 20 kPa.

Comparison with Stress-Strain Model

This section focuses on evaluating whether the typical bi-log-linear model applied to the compression of soils (e.g., Das and Sobhan 2018) could be applied to Type B TDA. The input parameters are the compression index C_c, the recompression index C_r, the initial specimen height H, the initial void ratio e_o, the yield stress σ'_c, the initial effective stress σ'_o, and the variation of effective stress $\Delta\sigma$. The settlement S is calculated as follows when $\sigma'_o + \Delta\sigma' < \sigma'_c$:

(Eq. 1) $$S = \frac{C_r H}{1 + e_o} log\left(\frac{\sigma'_o + \Delta\sigma'}{\sigma'_o}\right)$$

and as follows when $\sigma'_o + \Delta\sigma' > \sigma'_c$:

(Eq. 2) $$S = \frac{C_r H}{1 + e_o} log\left(\frac{\sigma'_c}{\sigma'_o}\right) + \frac{C_c H}{1 + e_o} log\left(\frac{\sigma'_o + \Delta\sigma'}{\sigma'_c}\right)$$

The results and comparison of the model with the experimental data is presented in Figure 7.

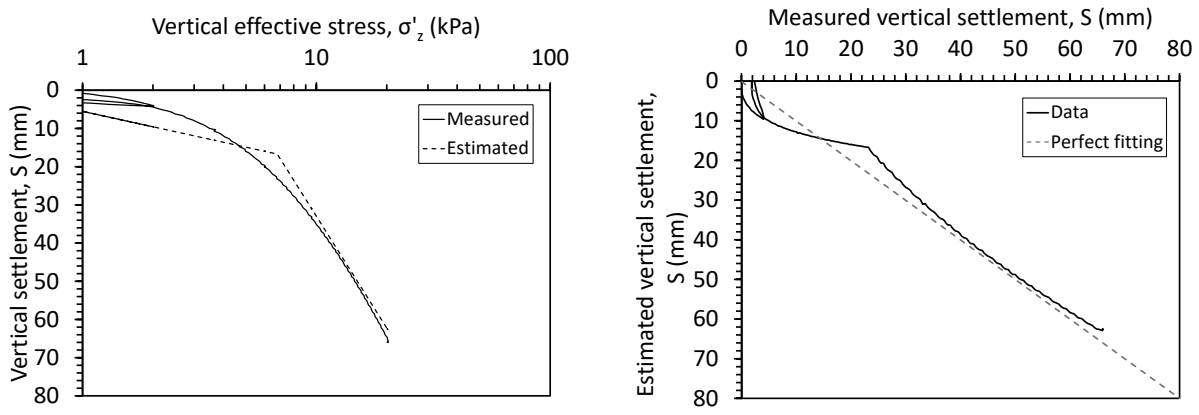

(a) **(b)**

Figure 7. Comparison with bi-log-linear model: (a) Stress-Strain curve, and (b) Direct comparison of model and experimental data.

The model slightly overestimates the one-dimensional compression at low stresses as shown in Figure 8. However, once the effective vertical stress approaches the apparent yield stress, this behavior is inverted. It is important to note that the compression curve of the Type B TDA on a natural scale in Figure 5(a) is not completely linear but does not show a clear point of yielding, so the nonlinear shape in Figure 7(a) can partly be attributed to the log scale. Beyond the apparent yield stress, the model predicts the one-dimensional compression with considerable accuracy until the end of the compression stage. Overall, the bi-log-linear model estimates the one-dimensional compression with reasonable accuracy for the Type B TDA at the studied initial unit weight of the TDA evaluated, but a challenge will be in the estimation of the apparent yield stress in the bi-log-linear model. A continuous compression curve relationship could also be investigated in future research to avoid having to define an apparent yield stress value.

Creep

Creep or time-dependent compression was investigated on the Type B TDA specimen subjected to constant vertical effective stress of 20.4 kPa over a period of 1 hour. The creep was tested during the same test as the one-dimensional compression test. Once the one-dimensional compression test reached the peak vertical load, the load was set constant for the time previously mentioned. Figure 8 presents the time-strain curve for the constant load stage. A typical tool to address the creep behavior of soil materials in engineering practice is the modified secondary compression

index $C_{\alpha\varepsilon}$ (Wartman et al. 2007). The parameter ($C_{\alpha\varepsilon}$) is defined as follows and is computed based on this study's results:

(Eq. 3) $$C_{\alpha\varepsilon} = \frac{\Delta\varepsilon_v}{\log\left({}^{t_2}/_{t_1}\right)}$$

where $\Delta\varepsilon_v$ is the change in time-dependent volumetric strain, t_1 is the time when time-dependent compression begins, t_2 and is the time at which the magnitude of the time-dependent compression requires to be estimated.

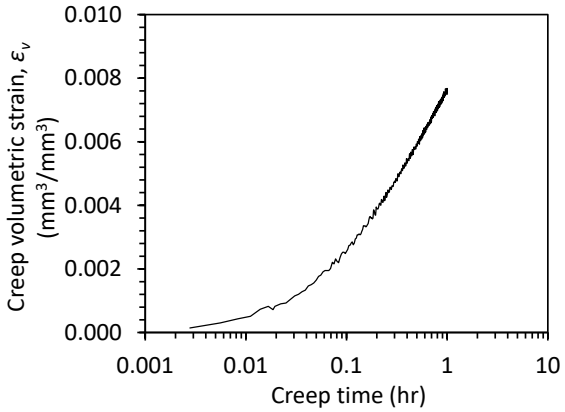

Figure 8. Creep volumetric strain versus time for Type B TDA under σ' = 20.4 kPa.

The results shown in Figure 8 indicate that the volume of the Type B TDA specimen decreases non-linearly over time, with the largest volume change occurring during the first minutes of the constant load. The TDA material seems to be stabilizing over time. The modified secondary compression index $C_{\alpha\varepsilon}$ computed in this study is 0.0029. In practice, creep or time-dependent compression is typically addressed by waiting eight weeks after the TDA placement before the placement of the settlement-sensitive components (Wartman et al. 2007). The computed parameter ($C_{\alpha\varepsilon}$) suggests that this practice could be satisfactory for the typical Type B TDA embankments. Nonetheless, more investigation about the creep at longer periods and at different vertical effective stresses than the ones considered at this study is encouraged to confirm this information.

CONCLUSIONS

This paper presents results from an oedometer test performed to characterize the one-dimensional compression and creep response of an 810 mm-thick layer of Type B TDA under static uniaxial compressive stresses in a large-scale rigid container having a length of 5,029 mm and a width of 2,184 mm. The one-dimensional compression behavior of the Type B TDA yields a non-linear stress-strain relationship during loading and unloading. The computed compression and recompression indices for a fitted bi-log-linear compression curve are 0.32 and 0.04, respectively. It also found the bi-log-linear model used for soils implemented with the compression index and swell index computed in this study has adequate accuracy for describing the compression response of Type B TDA under the vertical effective stresses considered in this study, although further

research is needed to understand the role of initial unit weight on the yield stress. The comparison with similar studies indicates that Type B TDA is less compressible during the initial compression stage (at low effective stress), and more compressible during the main compression stage than Type A TDA under vertical effective stresses larger than 20 kPa. The creep behavior investigation of the Type B TDA indicated that the volume of the material decreases over time with the highest volumetric strain change occurring during the first minutes of the constant load. The results allowed the computation of the modified secondary compression parameter as 0.0029.

ACKNOWLEDGEMENTS

Support for this study provided by CalRecycle under agreement DRR19090 is gratefully acknowledged. The authors thank Joaquin Wright of GHD and Stacey Patenaude of CalRecyle for their support. The authors also thank Andrew Sander, Michael Sanders, Noah Aldrich, Michael Dyson, Christopher Latham, Rebecca Bauman, Pablo Garcia, Zackary Kamibayashiyama, and Alejandro Ibarra, for their input and support during construction and testing of the specimen.

REFERENCES

ASTM. (2011). *Standard Test Methods for One-dimensional Consolidation Properties of Soils Using Incremental Loading*. ASTM D2435-04, West Conshohocken, PA

ASTM. (2012). *Standard Practice for Use of Scrap Tires in Civil Engineering Applications*. ASTM D6270, West Conshohocken, PA

Bosscher, P.J., Edil, T.B., and Eldin, N.N. (1992). "Construction and performance of a shredded waste tire test embankment." *Transportation Research Record 1345*, Transportation Research Board, Washington, DC, 44–52.

CalRecycle (California Department of Resources Recycling and Recovery) (2016). "California waste tire market report: 2015." *DRRR 2016-01567, Sacramento, CA.*

Das, B.M. and Sobhan, K. (2018). *Principles of Geotechnical Engineering*, 9th edition. CENCAGE learning. Boston, MA, USA.

Dickson, T.H., Dwyer, D.F., and Humphrey, D.N. (2001). "Prototype tireshred embankment construction." *Transp. Res. Rec*., 1755, 160–167.

Drescher, A., and Newcomb, D.E. (1994). "Development of design guidelines for use of shredded tires as a lightweight fill in road subgrade and retaining walls." *Report No. MN/RC-94/04*, Dept. of Civil and Mineral Engineering, Univ. of Minnesota, Minneapolis.

Edeskar, T. (2004) "Technical and environmental properties of tire shreds focusing on ground engineering applications" SE-971 87 Lulea, Dept. of Civil and Mining Engineering, Lulea University., Lulea, Sweden.

Feng, Z.Y., and Sutterer, K.G. (2000). "Dynamic properties of granulated rubber/sand mixtures." *Geotech. Test. J*., 23(3), 338–344.

Fox, P.J., Sanders, M., Latham, C., Ghaaowd, I., and McCartney, J.S. (2017), "Large-scale direct-simple shear test for large-particle tire-derived aggregates" *Geotech. Test. J*., 04017079.

Ghaaowd, I., McCartney, J.S., Thieltmann, S.S., Sanders, M.J., and Fox, P.J. (2017) "Shearing behavior of tire-derived aggregate with large particle size. I: Internal and Concrete Interface Direct Shear." *Journal of Geotechnical and Geoenvironmental Engineering* 143, no. 10: 04017078. https://doi.org/10.1061/(ASCE)GT.1943-5606.0001775.

Hoppe, E.J. (1994). “Field study of shredded-tire embankment.” *Report No. FHWA/VA-94-IR1*, Virginia Dept. of Transportation, Richmond, VA.

Humphrey, D.N. (2008a). “Civil engineering application of tire derived aggregate.” Alberta Recycling Management Authority, Edmonton, AB, Canada.

Humphrey, D.N. (2008b). “Tire derived aggregate as lightweight fill for embankments and retaining walls.” Department of Civil and Environmental Engineering, University of Maine. Orono, Maine. USA.

Humphrey, D.N., and Manion, W.P. (1992). “Properties of tire chips for lightweight fill.” *Proc., Grouting, Soil Improvement, and Geosynthetics*, ASCE, New York, 1344–1355.

Meles, D., Bayat, A., and Soleymani, H., (2013). “Compression behavior of large-sized tire-derived aggregate for embankment application”

Mills, B., and McGinn, J. (2010). “Design, construction, and performance of highway embankment failure repair with tire-derived aggregate.” *Transportation Research Record 1345*, Transportation Research Board, Washington, DC, 90–99.

Tandon, V., Velazco, D.A., Nazarian, S., and Picornell, M. (2007). “Performance monitoring of embankment containing tire chips: Case study.” *J. Perform. Constr. Facil.*, 21(3), 207–214.

Tweedie, J.J., Humphrey, D.N., and Sandford, T.C. (1998). “Full scale field trials of tire shreds as lightweight retaining wall backfill, at-rest condition.” Transportation Research Board, Washington, DC.

Wartman, J., Natale, M. F., and Strenk, P. M. (2007). “Immediate and time-dependent compression of tire derived aggregate.” *Journal of Geotechnical and Geoenvironmental Engineering* 133, no. 3: 245–56. https://doi.org/10.1061/(ASCE)1090-0241(2007)133:3(245).

Yarahuaman, A. and McCartney, J.S. (2022). “Seismic response of rail embankments.” Proc. GeoCongress 2022. Charlotte. Mar. 20-23. GSP 336, ASCE, Reston, VA. 300-310. https://doi.org/10.1061/9780784484067.031